

Lead zirconate titanate multi-element structure by electrophoretic deposition

A.-P. Abellard^{1, 2, 3}, D. Kuščer^{2, 4}, M. Lethiecq¹, J.-M. Grégoire⁵, B. Malič² and F. Levassort¹

¹Université François-Rabelais de Tours, CNRS, CEA, ENIVL, GREMAN UMR 7347, site ST Microelectronics, Tours, France

²Jožef Stefan Institute, Ljubljana, Slovenia

³Jožef Stefan International Postgraduate School, Ljubljana, Slovenia

⁴Centre of Excellence NAMASTE, Ljubljana, Slovenia

⁵Université François-Rabelais de Tours, UMR Imagerie et Cerveau, Inserm U930, Tours, France

Abstract: Processing of aligned piezoelectric elements for multi-element linear-array transducers was studied. Transducers consist of six rectangular elements with a length of about 6 mm, a width of 1.1 mm and a distance between them of about 0.4 mm. Lead zirconate titanate (PZT) elements were prepared on metalized alumina substrates by electrophoretic deposition (EPD) process and sintering. PZT and PbO particles were dispersed in ethanol and deposited on the substrate at a constant current. After the sintering at 950°C, uniform elements with a thickness of around 20 µm and a density around 83 % were obtained. The space between elements, i.e., a kerf, was filled with an epoxy resin. Electrical contacts of each element were performed using wedge bonding and a six element structure was electromechanically characterized. A thickness mode coupling factor (kt) of around 17 %, a resonance frequency of around 70 MHz (in free mechanical conditions), a dielectric constant of around 370 were measured. A good reproducibility was observed. Limitations of the EPD method in terms of spatial resolutions for patterning very small piezoelectric elements are discussed and results show that EPD is a promising process for high frequency linear array applications.

This work is dedicated to the late Professor Marija Kosec

Keywords: Electrophoretic deposition, piezoelectric thick film, multi-element transducer, ultrasound applications.

Večelementna struktura svinčev cirkonat titanat z elektroforetskim nanosom

Izvleček: Študirali smo pripravo piezoelektričnih elementov za ultrazvočne pretvornike. Pretvornik je bil sestavljen iz linearnega niza šestih elementov z dolžino 6 mm in širino 1 mm, razdalja med posameznimi elementi je bila 0.5 mm. Elemente na osnovi svinčevega cirkonata titanat (PZT) smo pripravili na metalizirani korundni podlagi z metodo elektroforetskega nanosa (EPD). Delce PZT in svinčevega oksida smo dispergirali v etanolu ter jih v ustreznem stehiometričnem razmerju z EPD nanесли na podlago pri konstantnem toku. Po žganju pri 950°C so imeli elementi debelino okoli 20 µm, homogeno mikrostrukturo in gostoto okoli 83 %. Presledke med posameznimi elementi (ang. kerf) smo zapolnili z epoksidno smolo, nanесли zgornjo elektrodo ter izmerili elektromehanske lastnosti posameznih elementov. Povprečni sklopitveni faktor piezoelektričnega elementa je bil 17 %, dielektrična konstanta okoli 370 in resonančna frekvenca okoli 70 MHz. Rezultati meritev posameznih elementov so bili podobni. V prispevku poročamo tudi o možnostih oblikovanja debeloplastnih struktur z EPD ter navajamo omejitve metode predvsem s stališča ločljivosti. Rezultati raziskave so pokazali, da je opisana metoda primerna za pripravo visokofrekvenčnih pretvornikov, sestavljenih iz linearnega niza piezoelektričnih elementov.

Ključne besede: Elektroforetski nanos, piezoelektrične debele plasti, ultrazvočni pretvorniki, ultrazvok

* Corresponding Author's e-mail: andre-pierre.abellard@univ-tours.fr

1 Introduction

Ultrasound techniques are widely used for non-destructive testing as well as medical investigations. For imaging small biological structures such as skin and eyes, the ultrasonic transducers have to operate at frequencies over 20 MHz to reach spatial resolutions lower than 100 micrometers [1-2].

High frequency (HF) single element transducers were extensively studied. These transducers consist of few tens of micrometers thick piezoelectric elements deposited onto a mechanical support. The piezoelectric material is the most important component of the transducer because its characteristics together with its geometry mainly define the properties of the transducer, in particular its operating frequency and sensitivity [3].

Transducers with good performance were obtained using different technologies for the piezoelectric thick film fabrication such as screen-printing [4-6], pad printing [7-9] and composite sol-gel [10-12], in a wide range of frequencies from 15 to 70 MHz. The main disadvantages of single element transducers are a fixed focal distance which leads to a limited depth of field. Moreover, to perform mode-B imaging [13], the transducer must be inserted into a probe which ensures a mechanical movement. Consequently, a limited frame rate is obtained.

Since the early 2000's, high-frequency multi-element transducers have been studied and developed.

Annular arrays [14-15] with typically 5 to 8 ring-shaped elements are used and a variable focal distance is obtained by changing the delays applied on the electrical excitation and received signals. However, the mechanical movement is always required. Linear arrays consist of a higher number of elements, e.g., 64, 128 or 256, but scanning and focusing are completely managed by electronics. However, the technological implementation of such transducers is much more complex [16-17]. In particular, the fabrication of the multilayer structure (backing, piezoelectric layer with elements and matching layers) is a challenge mainly due to the micrometer-size of rectangular piezoelectric elements with a thickness of few tens of micrometers. As an example, for a linear array transducer operating at 50 MHz, an element width around 25 μm , a space between elements (kerf) around 10 μm and a thickness around 30 μm are needed [18]. Cannata *et al* [19] designed a kerfless linear array transducer to simplify its fabrication procedure. Their design was based on a uniform piezoelectric layer. The individual elements were obtained simply by shaping the bottom electrode or the top electrode or both. However, they reported that the crosstalk between el-

ements was significant both electrically and mechanically, which reduces the performance of the transducer and in particular the piezoelectric element directivity [20]. Foster *et al.* [21] used laser-machining to dice and sub-dice the elements from a piezoelectric layer to fabricate a HF linear array with very low kerf value. They prepared an efficient linear array transducer with 256 elements that was operated at a resonant frequency of 40 MHz.

1-3 or 2-2 piezo-composites were also used as the piezoelectric layer for high frequency linear array fabrication [22-23]. In such structures, cross-talk is naturally reduced and kerfless structure or partial cuts between elements were used. Moreover, due to polymer content, the piezocomposite is flexible, which is often used to obtain geometric focusing along the elevation [24-26]. At frequencies above 20 MHz, the typical size of the periodic microstructure of a composite (alternatively constituted of piezoelectric rods or layers and polymer) must be very low, typically around ten micrometers. Good performance was obtained but required highly technical and costly processes.

Recently, electrophoretic deposition (EPD) was used to process piezoelectric thick films on a complex-shape substrate and thus to fabricate efficient, geometrically-focused single element transducers [27]. EPD is an adaptive and low cost method enabling the deposition of various materials on a complex-shape conductive substrate. The charged particles dispersed in a solvent can be deposited on an electrode, e.g., a metalized substrate, by applying a DC electric field between it and a counter-electrode [28-30]. To process piezoelectric thick films with desired microstructure and functional response, the properties of the suspension, the deposition process as well as the drying and sintering procedure have to be optimized [31].

The purpose of the present study was to deposit rectangular piezoelectric elements for high frequency transducers with a straightforward procedure to test the compatibility of electrophoretic deposition with the development of a high frequency linear array.

We report here the results on patterning of lead zirconate titanate thick film structures by EPD and consequent sintering. The simple prototype linear array transducer consisting of six piezoelectric elements, has been prepared. The electromechanical properties in thickness mode of each individual element were measured. Finally, the use of EPD to fabricate array elements with very small sizes originally defined in 2D thanks to conductive electrodes is evaluated and quantified.

2 Experimental procedure

2.1 Substrate preparation and thick film fabrication

Dense alumina substrates, namely Al_2O_3 (Kyocera A493) with dimensions 12 mm x 12 mm and a thickness of 640 μm were used. A gold paste (8884-G, ESL) was screen-printed onto the Al_2O_3 and fired at 900°C for 10 min to deliver six aligned rectangles with a length of 6 mm, a width of 1 mm and a space between them of 500 μm . These golded substrates are denoted $\text{Au}/\text{Al}_2\text{O}_3$. A photograph of the electroded substrate is presented in Figure 1. The acoustical properties of dense alumina are reported elsewhere [32]. Additional gold lines were screen-printed at the same time to simplify the electrical contact for the future transducer fabrication.

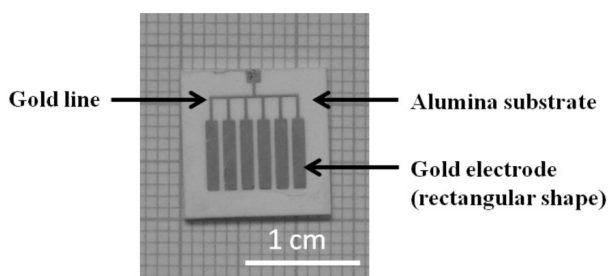


Figure 1: Representative $\text{Au}/\text{Al}_2\text{O}_3$ structure consisting of 6 aligned rectangular gold electrodes with a length of 6 mm, a width of 1 mm and a space between electrodes of 500 μm .

$\text{Pb}(\text{Zr}_{0.53}\text{Ti}_{0.47})\text{O}_3$ powder (PZT) was prepared by solid state synthesis from PbO (99.9+ %, Aldrich), ZrO_2 (99.9 %, Tosoh) and TiO_2 (99.9 %, Alfa Aesar). The homogeneous mixture was calcined at 950 °C. After the calcination the powder was milled for 8 h in an attritor mill. Details are given in [33].

PZT and PbO suspension with a solid load content of 1 vol. % was prepared. PZT and PbO particles were dispersed in ethanol using polyacrylic acid (PAA, Alfa Aesar, M_v 2000) and n-butylamine (BA, Alfa Aesar). The procedure is reported in [33]. The suspension for EPD was prepared by mixing PZT and PbO suspensions in stoichiometry 98 mol % PZT and 2 mol % PbO and is denoted as PZT- PbO .

The zeta-potentials of PZT and PbO particles in ethanol were measured at room temperature using a ZetaPals zeta-potential analyzer (Brookhaven Instruments). The conductivity of the suspension was measured at room temperature using a Cond 730 Inolab system.

EPD was performed at room temperature in a horizontal electrode cell with two $\text{Au}/\text{Al}_2\text{O}_3$ identical sub-

strates, acting as a cathode and an anode. The distance between the electrodes was 25 mm. The area of the whole conductive surface was 42 mm^2 . The deposition was performed at a constant current density of 2.38 mA/cm^2 for 40 sec using a Keithley 2400 generator (Keithley Instruments Inc., Cleveland, USA).

The as-deposited layers were sintered at 950°C for 2 hours with heating and cooling rates of 2°C/min in a lead oxide rich atmosphere provided by $\text{PbZrO}_3/\text{PbO}$ packing powder.

The thickness and the surface of as-deposited dried layers were investigated by a profilometer (Viking 100 Solarius Inc.).

The microstructures of sintered thick films were characterized with a scanning electron microscope (SEM) (JEOL 5800, Japan). The microstructure was prepared by cutting samples into two pieces and mounting them in parallel in epoxy resin, grinded and polished. A small layer of carbon was deposited on the top of the microstructure in epoxy.

The density of the sintered thick film was obtained by a quantitative characterization of the ceramic microstructure. This characterization was obtained from SEM images converted to binary ones using an image analysis software (ImageTools 3.0, University of Texas Health Science Center, USA) to determine the volume fraction of pores [34]. We quantified the black and white pixels of the binary images and calculated the percentage of the porosity by dividing the number of black pixels by their total amount. An experimental error of ± 3 % is estimated.

2.2 Preparation and characterization of the prototype

After sintering, the spaces (kerfs) between piezoelectric elements were filled with epoxy resin. To perform the electromechanical characterization, a 100 nm thick top gold electrode was sputtered on the whole area of the sample. The six-element structure was poled at 150°C for 10 min in an oil bath with an electric field of 6 kV/mm .

After poling, the six elements numbered 1-6 were electrically separated and the structure was glued on a Printed Circuit Board (PCB) substrate with additional copper connection to facilitate electrical contacts. The electrical connections between copper lines and elements through gold wires were performed by wedge bonding. Finally, epoxy resin was added on the gold wires to protect these connections. A photograph of the demonstrator is shown in Figure 2.

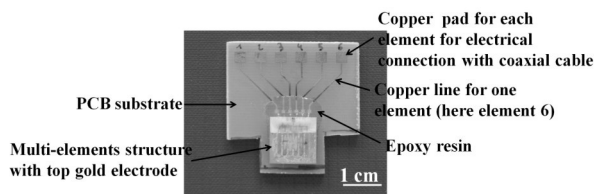


Figure 2: Photograph of the demonstrator.

The electromechanical properties of the piezoelectric thick film structures were deduced from the measurement of the complex electrical impedance around the fundamental thickness mode resonance. A HP 4395 vector analyzer and an impedance test kit were used. The theoretical behavior of the electrical impedance was computed as a function of frequency for the thickness mode using a one-dimensional model based on the KLM equivalent electrical circuit [35-36]. Then a fitting process was used to deduce the thickness mode parameters of the EPD piezoelectric thick films from the experimental data [6, 12, 37].

For one piezoelectric element, the structure along the thickness is composed of four layers, *i.e.*, three passive and the active thick film. The passive layers are the alumina substrate and the two gold electrodes. The parameters of these layers are fed in the KLM model and considered as constants [9, 32]. Parameters for the flat alumina substrate are given in [27].

Finally, five thickness mode parameters of the thick film were deduced: the longitudinal wave velocity v_l , the dielectric constant at constant strain $\epsilon_{33}^S/\epsilon_0$, the effective thickness coupling factor k_t and the loss factors (mechanical δ_m , electrical δ_e).

For the measurement of the electroacoustic responses of the elements, a 50 Ohms coaxial cable with a length of around 30 cm, was used. Two electrical contacts were performed. One on the copper pad (see Figure 2) corresponding to the desired piezoelectric element and the other on the top gold electrode, which is common for all elements using conductive epoxy resin. Each element was characterized in pulse-echo mode on a brass target in water. An AVTEC AVG-3B -C impulse generator (Avtech Electrosystems Ltd., Ottawa, Canada) was used for the electrical excitation. Reception was performed with a home-made high frequency receiver.

3 Results and discussion

For EPD, the suspension that contains PZT and PbO particles dispersed in an ethanol was used. The zeta potential of -50 ± 5 mV and -40 ± 5 mV were obtained for PZT and PbO, respectively. The conductivity of PZT-PbO suspension was $18 \mu\text{S}/\text{cm}$ at 24°C . The high negative

value of the zeta potential indicates that the negatively charged particles are well dispersed in a solvent. The low value of the conductivity is favorable for the deposition process [38]. During the EPD process, the piezoelectric layer is deposited onto the positively charged Au/Al₂O₃ substrate.

The uniformity of the as-deposited six elements on Au/Al₂O₃ was investigated by a profilometer. The image and the profile in A-A direction are shown in Figure 3a and b, respectively. From the profile image, it is evident that the edges of all the lines are thicker than their centers. The variations in the thickness may be related to the non-uniform electric field applied during the EPD. In between the lines we have not detected any deposit. No micro defects such as cracks were observed. The as-deposited elements had a thickness around 50 micrometers

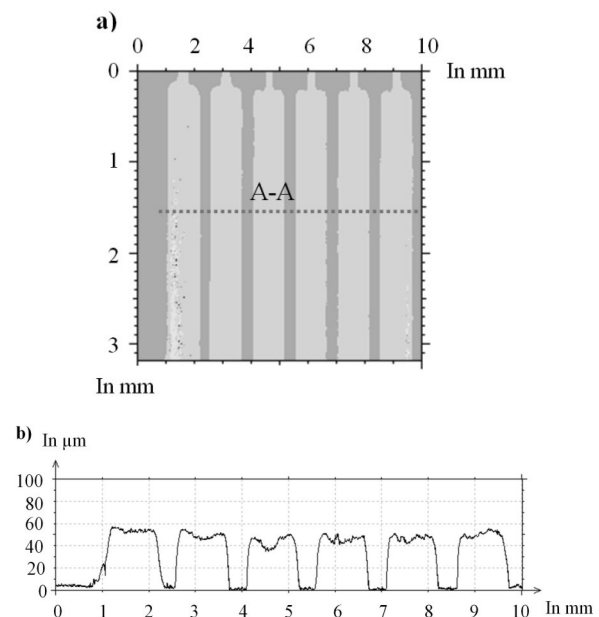


Figure 3: a) Image of the six as-deposited elements on Au/Al₂O₃. b) Profile of the six as-deposited elements on Au/Al₂O₃ measured by profilometer.

The sintered samples were analyzed by SEM in order to determine precisely the thickness of the elements, their width and the kerf. Microstructures of PZT-PbO elements in cross-sectional orientation sintered at 950°C are shown in Figure 4. Good adhesion between PZT-PbO and Au/Al₂O₃ is evident and no delamination of electrode and/or PZT-PbO from the substrate was detected.

The thickness of the film is not uniform and varies from about $18 \pm 3 \mu\text{m}$ in the middle to about the $30 \pm 3 \mu\text{m}$ at the edge of the elements as evident from the Figure 4. The thickness is based on the measurement of six elements and the average value is given. It is also seen

that the PZT elements were wider than the size of the gold bottom electrode of about 100 μm. Consequently, a kerf around 400 μm was measured. From Figure 4c it is evident that the PZT-PbO is homogeneous and consists of micrometer sized grains. The density of the layer calculated by stereological analysis was 6.640 g/cm³, corresponding to 83 ± 3 % of the theoretical density.

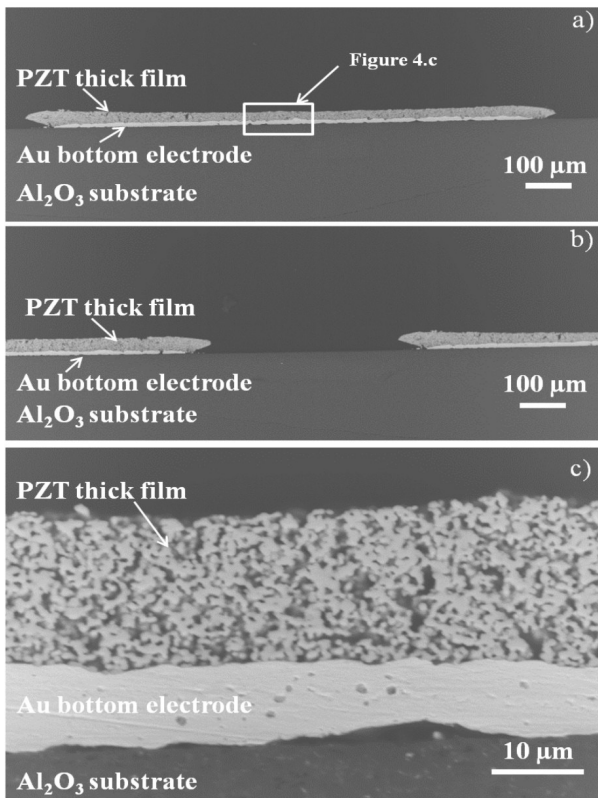


Figure 4: PZT-PbO thick films on a flat Au/Al₂O₃ substrate sintered at 950 °C for 2 h. SEM cross section image of a) one element; b) two elements and kerf in the middle. c) Inset from Figure 1a) (magnification x 2000)

3.1 Electromechanical properties of the structure

Impedance measurements were performed on the 6 elements. For the first two elements (numbered 1 and 2), electrical connections were strongly degraded and measurements were not exploitable. Consequently, experimental results from elements 3 to 6 were used. Figure 5 represents the electrical impedances (experimental and theoretical) in air of a representative element in the structure.

The extracted parameters from impedance curves of the 4 elements are summarized in Table I. For the calculation, we used the thickness measured at the center of the element (which represents the majority of the whole element area), which was about 20 μm. The results were compared to those on sample “Ref_PZT-

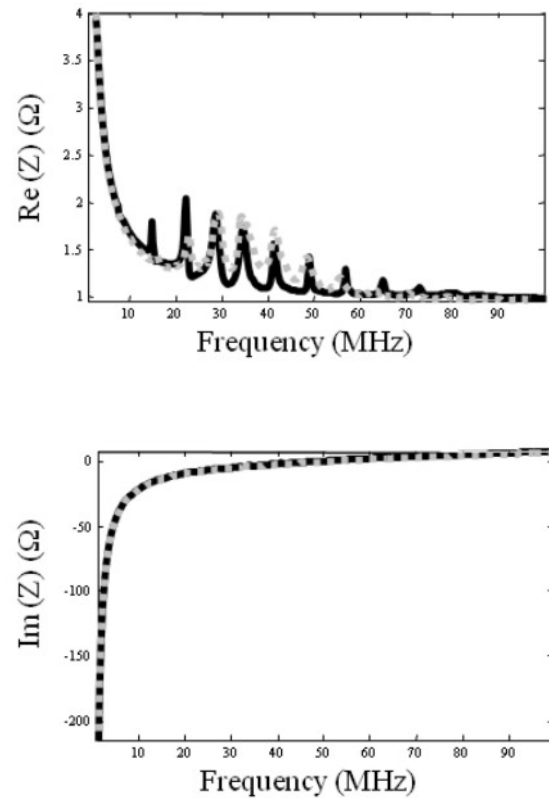


Figure 5: Complex electrical impedance of one element (number 5) in air as a function of frequency around the fundamental resonance (black solid line: theoretical, gray dashed line: experimental).

PbO” published in a previous study [39]. The “Ref_PZT-PbO” thick film was prepared from the same suspension as the multi-element structure in this study. It was deposited at identical conditions, i.e., for 60 sec on a surface of 64 mm². After the sintering, the thickness of the sample was uniform, i.e., 20 μm, and a density of 83 ± 2 % was found.

Table 1: *t*: thickness, *v_l*: the longitudinal wave velocity, $\epsilon_{33}^S / \epsilon_0$: dielectric constant at constant strain, δ_m : mechanical losses, δ_e : dielectric losses, *f₀*: thick film resonance frequency (in free mechanical conditions).

Sample	<i>t</i> (μm)	<i>v_l</i> (m/s)	<i>k_t</i> (%)	$\epsilon_{33}^S / \epsilon_0$	δ_m (%)	δ_e (%)	<i>f₀</i> (MHz)
Element 3	20	2850	17	360	22	3	71
Element 4	19	2790	17	350	17	3	70
Element 5	20	2900	20	410	20	3	72
Element 6	20	2850	15	390	17	3	71
Ref_PZT-PbO ([39])	20	2780	48	320	6	1	69

The four elements have a higher longitudinal wave velocity and dielectric constant than the PZT-PbO thick film considered as reference [39].

A lower porosity content in the four elements can explain these differences. Mechanical losses were also significantly higher in the four elements than in the reference sample. This could be explained by the non-uniformity of the thickness of the four elements. Indeed, when using the KLM model to extract parameters, a constant thickness was assumed; consequently, mechanical losses were overestimated.

The main difference observed between the four elements and the reference sample was the thickness coupling factor which was about $17 \pm 2 \%$ for the four elements, while it was 48 % for the reference sample. The higher k_t for the reference samples may be related to the more efficient pooling that was performed at 12 kV/mm. The electric field of 6 kV/mm was evidently too low, therefore the poling procedure for the piezoelectric rectangular elements must be optimized. Finally, it is also important to notice the good reproducibility of the electromechanical properties and dimensions measured on the four elements. This reproducibility attests that linear arrays with higher number of element are feasible by such a process.

3.2 Electroacoustic response of a representative element

Figure 6 a represents the pulse-echo response of a representative element (number 5). In this configuration, only one element is excited while other elements stay with floating electric potential. The sensitivity $S = 20 \cdot \log_{10} (U_e / U_r)$, where U_e and U_r are the excitation and reception peak voltages, was evaluated from the received voltage in pulse-echo mode. The sensitivity was -45 dB. The bandwidth at -6 dB deduced from the frequency response (Figure 6.b) has a value of 16 MHz and a center frequency of 42 MHz (which corresponds to a fractional bandwidth at -6dB of 38 %). These delivered electro-acoustic properties confirm the high potential of the EPD process. But in this configuration, the alumina substrate was not an ideal material to be used as backing for three main reasons. The attenuation in this material is low (typically 0.06 dB.mm [32]) and the thickness of the substrate is not sufficiently high to avoid back wall echoes. In fact, Figure 6 a represents only the first echo corresponding to the electro-acoustic response of the structure, but additional echoes follow due to multiple reflections in the substrate. Moreover, acoustical impedance of the alumina substrate is twice that of the piezoelectric element and this large difference limits the bandwidth of the electro-acoustic response. For medical imaging applications, a bandwidth higher than 50 % is required. In the future, a material with sufficiently high attenuation and lower acoustical impedance must replace alumina substrate. Unpoled porous PZT material is a viable option for properties and compatibility with the EPD pro-

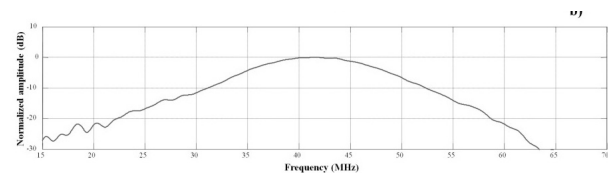
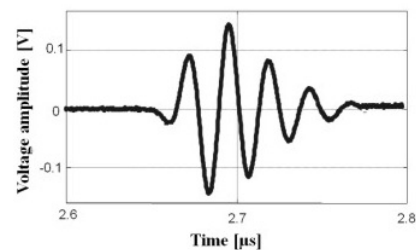


Figure 6: Experimental electro-acoustic responses for the element number 5 of the multi-element structure. (a) time response and (b) frequency response.

cess. This material was already used for single element transducers [6]. For this study, the objective was to demonstrate the potential of the EPD process and the alumina substrate was chosen in order to guarantee a good accuracy for the measured electromechanical properties (typically the thickness coupling factor) [12].

4 Conclusions

The electrophoretic deposition process was used for the fabrication of piezoelectric PZT-PbO thick films on flat Au/Al₂O₃ substrates for ultrasonic high frequency linear array configurations. After the sintering, the piezoelectric elements had a rectangular shape with a width of 1.1 mm and a kerf of 400 μm. The thickness of the films of around 20 μm delivered ultrasound frequencies over 30 MHz, which is well adapted to high resolution medical imaging applications.

The elements are characterized by a dielectric constant of 370, a coupling factor around 17 % and a longitudinal wave velocity around 2800 m/s. For an optimized high frequency linear array configuration, the width of elements and kerf need to be significantly reduced as mentioned in the introduction. The most critical step will be to minimize the kerf value to a few tens of micrometers while keeping the “Π shape” of the elements. For that, several routes are already planned and a modified experimental protocol for EPD will be tested. The electromechanical performance of all elements is similar but still needs to be improved by optimizing the poling conditions. Nevertheless, high reproducibility of elements in terms of shape and performance suggests that EPD can be considered as a promising process for the fabrication of high frequency linear arrays.

5 Acknowledgments

The authors are grateful for the financial support of the Slovenian Research Agency (Research Programme P2-0105) and the University François-Rabelais of Tours.

The authors are grateful for technical assistance of Vermon S.A. (Claire Bantignies).

The authors would like thank Mr. Silvo Drnovsek for technical assistance, Mrs. Jena Cilensek for preparation of the microstructures, and Mr. Jean-Yves Tartu and Marie Perroteau for assistance with the transducer fabrication.

The contribution of Prof. Dr. Marija Kosec who passed away in December 2012 is acknowledged with gratitude.

6 References

1. F. S. Foster, C. J. Pavlin, K. A. Harasiewicz, D. A. Christopher and D. H. Turnbull *Advances in ultrasound biomicroscopy*. Ultrasound in medicine & biology, 2000, 26(1): p. 1-27.
2. K. K. Shung, J. M. Cannata and Q. F. Zhou *Piezoelectric materials for high frequency medical imaging applications: A review*. Journal of Electroceramics, 2007, 19(1): p. 139-145.
3. M. Lethiecq, F. Levassort, D. Certon and L. P. Tran-Huu-Hue, *Piezoelectric Transducer Design for Medical Diagnosis and NDE*. Piezoelectric and Acoustic Materials for Transducer Applications, Ed. 2008. Chap. 10: p. 191-215.
4. H. Janez, M. Kosec, F. Levassort, L. Tran-Huu-Hue and M. Lethiecq *Integrated ultrasonic piezoelectric transducers for medical applications*. Informacije MIDEM, 2003, 33(1): p. 53-56.
5. M. Lethiecq, F. Levassort and L. Tran-Huu-Hue *Ultrasonic transducers for high resolution imaging: from piezoelectric structures to medical diagnostics*. Informacije Midem, 2005, 35(4): p. 177-186.
6. P. Marechal, F. Levassort, J. Holc, L.-P. Tran-Huu-Hue, M. Kosec and M. Lethiecq *High-frequency transducers based on integrated piezoelectric thick films for medical imaging*. IEEE Transactions on Ultrasonics, Ferroelectrics and Frequency Control, 2006, 53(8): p. 1524-1533.
7. G. Love, G. Maher and N. Long, *Pad printer*. Electronics Manufacturing Technology Symposium, 1996.
8. M. Lethiecq, R. Lou-Moeller, J. A. Ketterling, F. Levassort, L. P. Tran-Huu-Hue, E. Filoux, R. H. Silverman and W. W. Wolny *Non-planar pad-printed thick-film focused high-frequency ultrasonic transducers for imaging and therapeutic applications*. Ultrasonics, Ferroelectrics and Frequency Control, IEEE Transactions on, 2012, 59(9): p. 1976-1982.
9. E. Filoux, R. Lou-Moeller, S. Callé, M. Lethiecq and F. Levassort *Optimised properties of high frequency transducers based on curved piezoelectric thick films obtained by pad printing process*. Advances in Applied Ceramics, 2013, 112(2): p. 75-78.
10. D. A. Barrow, T. E. Petroff and M. Sayer *Thick ceramic coatings using a sol gel based ceramic-ceramic 0-3 composite*. Surface and Coatings Technology, 1995, 76-77(1): p. 113-118.
11. R. A. Dorey and R. W. Whatmore *Electrical properties of high density PZT and PMN-PT/PZT thick films produced using ComFi technology*. Journal of the European Ceramic Society, 2004, 24(6): p. 1091-1094.
12. A. Bardaine, P. Boy, P. Belleville, O. Acher and F. Levassort *Improvement of composite sol-gel process for manufacturing 40µm piezoelectric thick films*. Journal of the European Ceramic Society, 2008, 28(8): p. 1649-1655.
13. T. L. Szabo, *Diagnostic ultrasound imaging*. 2004: Academic press series in Biomedical engineering Hartford, Connecticut.
14. J. Brown, C. Morton-Demore, F. S. Foster and G. R. Lockwood, *Performance of a 50 MHz annular array based imaging system*. IEEE International Ultrasonics Symposium, 2004: p. 760-763.
15. J. A. Ketterling, S. Ramachandran, O. Aiszábal and O. Aristizábal *Operational verification of a 40-MHz annular array transducer*. IEEE transactions on ultrasonics, ferroelectrics, and frequency control, 2006, 53(3): p. 623-630.
16. <http://www.visualsonics.com/>
17. C. Bantignies, P. Mauchamps, F. Levassort, T. Matéo, J.-M. Grégoire, R. Dufait and F. Ossant, *40 MHz piezo-composite linear array for medical imaging and integration in a high resolution system*. IEEE International Ultrasonics Symposium, 2011: p. 226-229.
18. L. Changgeng, Z. Qifa, F. T. Djuth and K. K. Shung *High-frequency (>50 MHz) medical ultrasound linear arrays fabricated from micromachined bulk PZT materials*. Ultrasonics, Ferroelectrics and Frequency Control, IEEE Transactions on, 2012, 59(2): p. 315-318.
19. J. M. Cannata, J. A. Williams and K. K. Shung, *A kerfless 30 MHz linear ultrasonic array*. 2005 IEEE International Ultrasonics Symposium, 2005: p. 109-112.
20. C. E. Morton and G. R. Lockwood, *Evaluation of kerfless linear arrays*. IEEE International Ultrasonics Symposium, 2002: p. 1257-1260.

21. F. S. Foster, J. Mehi, M. Lukacs, D. Hirson, C. White, C. Chaggares and A. Needles *A New 15–50 MHz Array-Based Micro-Ultrasound Scanner for Preclinical Imaging*. *Ultrasound in medicine & biology*, 2009, 35(10): p. 1700-1708.
22. J. M. Cannata, J. A. Williams, Q. F. Zhou, T. A. Ritter and K. K. Shung *Development of a 35-MHz piezo-composite ultrasound array for medical imaging*. *IEEE Transactions On Ultrasonics Ferroelectrics and Frequency Control*, 2006, 53(1): p. 224-236.
23. C. Bantignies, P. Mauchamp, G. Ferin, S. Michau and R. Dufait, *Focused 20 MHz single-crystal piezocomposite ultrasound array*. *IEEE International Ultrasonics Symposium (IUS)*, 2009 IEEE International, 2009: p. 2722-2725.
24. J. A. Brown, F. S. Foster, A. Needles and G. R. Lockwood, *A 40 MHz Linear Array based on a 1-3 Composite with Geometric Elevation Focussing*. 2006 IEEE International Ultrasonics Symposium, 2006: p. 256-259.
25. J. A. Brown, E. S. Foster, A. Needles, E. Cherin and G. R. Lockwood *Fabrication and performance of a 40-MHz linear array based on a 1-3 composite with geometric elevation focusing*. *IEEE Transactions On Ultrasonics Ferroelectrics and Frequency Control*, 2007, 54(9): p. 1888-1894.
26. C. Bantignies, E. Filoux, R. Rouffaud, M. Pham Thi, J.-M. Grégoire and F. Levassort, *Lead-free high-frequency linear-array transducer (30 MHz) for in vivo skin imaging*. *IEEE International Ultrasonics Symposium*, 2013.
27. A.-P. Abellard, F. Levassort, J.-M. Gregoire, M. Lethiecq, D. Kuscer, J. Holc and M. Kosec, *PZT thick films obtained by electrophoretic deposition (EPD) process for high frequency focused transducers*. *IEEE International Ultrasonics Symposium (IUS)*, 2012: p. 190-193.
28. P. Sarkar and P. S. Nicholson *Electrophoretic Deposition (EPD): Mechanisms, Kinetics, and Application to Ceramics*. *Journal of the American Ceramic Society*, 1996, 79(8): p. 1987-2002.
29. I. Corni, M. P. Ryan and A. R. Boccaccini *Electrophoretic deposition : From traditional ceramics to nanotechnology*. *Journal of the European Ceramic Society*, 2008, 28(7): p. 1353-1367.
30. B. Ferrari and R. Moreno *EPD kinetics: A review*. *Journal of the European Ceramic Society*, 2010, 30(5): p. 1069-1078.
31. L. Pardo, J. Ricote, M. Kosec, D. Kuscer and J. Holc, *Processing of Ferroelectric Ceramic Thick Films. Multifunctional Polycrystalline Ferroelectric Materials: Processing and Properties*, Ed. 2011. Chap. p. 39-61.
32. A. R. Selfridge *Approximate Material Properties in Isotropic Materials*. *IEEE Transactions on Sonics and Ultrasonics*, 1985, 32(3): p. 381-394.
33. A.-p. Abellard, D. Kuščer, J. Holc, F. Levassort, M. Lethiecq, M. Kosec and S.-. Ljubljana, *Fabrication and modeling of piezoelectric transducers for High-Frequency medical imaging*. 47th International Conference on Microelectronics, Devices and Materials and the Workshop on Organic Semiconductors, Technologies and Devices, September 28 - September 30, 2011, 2011.
34. D. Kuscer, J. Korzekwa, M. Kosec and R. Skulski *A- and B-compensated PLZT x/90/10: Sintering and microstructural analysis*. *Journal of the European Ceramic Society*, 2007, 27(16): p. 4499-4507.
35. R. Krimholtz, D. Leedom and G. Matthaei *New equivalent circuits for elementary piezoelectric transducers*. *Electronics Letters*, 1970, 6(13): p. 398-399.
36. S. J. H. Van Kervel and J. M. Thijssen *A calculation scheme for the optimum design of ultrasonic transducers*. *Ultrasonics*, 1983, 21(3): p. 134-140.
37. M. Lukacs, T. Olding, M. Sayer, R. Tasker and S. Sherrit *Thickness mode material constants of a supported piezoelectric film*. *Journal of applied physics*, 1999, 85(5): p. 2835-2843.
38. D. Kuscer, T. Bakarič, B. Kozlevčar and M. Kosec *Interactions between Lead-Zirconate Titanate, Polyacrylic Acid, and Polyvinyl Butyral in Ethanol and Their Influence on Electrophoretic Deposition Behavior*. *The journal of physical chemistry. B*, 2013, 117(p. 1651-1659).
39. D. Kuscer, A.-P. Abellard, M. Kosec and F. Levassort, *Piezoelectric Thick-Film structures for High-Frequency applications prepared by electrophoretic deposition*. *Processing and Properties of Advanced Ceramics and Composites V*, Ed. 2013. Chap. 16: p. 131-140.

Arrived: 30. 09. 2013

Accepted: 01. 02. 2014